Minor contribution of small thaw ponds to the pools of carbon and methane in the inland waters of the permafrost-affected part of the Western Siberian Lowland

Y. M. Polishchuk, A. N. Bogdanov, I. N. Muratov, V. Y. Polishchuk, A. Lim, R. M. Manasypov, L. S. Shirokova, O. S. Pokrovsky

ENVIRONMENTAL RESEARCH
LETTERS

LETTER • OPEN ACCESS

Minor contribution of small thaw ponds to the pools of carbon and methane in the inland waters of the permafrost-affected part of the Western Siberian Lowland

To cite this article: Y M Polishchuk *et al* 2018 *Environ. Res. Lett.* **13** 045002

Environmental Research Letters

LETTER

Minor contribution of small thaw ponds to the pools of carbon and methane in the inland waters of the permafrost-affected part of the Western Siberian Lowland

Y M Polishchuk[1,2], A N Bogdanov[1], I N Muratov[1], V Y Polishchuk[3,4], A Lim[6], R M Manasypov[5,6], L S Shirokova[5,7] and O S Pokrovsky[7,8]

1 Ugra Research Institute of Information Technology, Khanty-Mansiysk, 628011, Russia
2 Institute of Petroleum Chemistry, SB RAS, Tomsk, 634021, Russia
3 Tomsk Polytechnic University, 634050, Tomsk, Russia
4 Institute of Monitoring of Climatic and Ecological Systems, SB RAS, Tomsk, 634021, Russia
5 N. Laverov Federal Center for Integrated Arctic Research, Russian Academy of Science, Arkhangelsk, Russia
6 BIO-GEO-CLIM Laboratory, Tomsk State University, Tomsk, Russia
7 Geoscience and Environment Toulouse, UMR 5563 CNRS, University of Toulouse, Toulouse, France
8 Author to whom any correspondence should be addressed.

E-mail: oleg.pokrovsky@get.omp.eu

Keywords: permafrost, geoinformation systems, lake size-distribution, space images, greenhouse gases, emission

Supplementary material for this article is available online

OPEN ACCESS

RECEIVED
4 September 2017

REVISED
24 January 2018

ACCEPTED FOR PUBLICATION
19 February 2018

PUBLISHED
16 March 2018

Abstract

Despite the potential importance of small (< 1000 m^2) thaw ponds and thermokarst lakes in greenhouse gas (GHG) emissions from inland waters of high latitude and boreal regions, these features have not been fully inventoried and the volume of GHG and carbon in thermokarst lakes remains poorly constrained. This is especially true for the vast Western Siberia Lowland (WSL) which is subject to strong thermokarst activity. We assessed the number of thermokarst lakes and their size distribution for the permafrost-affected WSL territory based on a combination of medium-resolution Landsat-8 images and high-resolution Kanopus-V scenes on 78 test sites across the WSL in a wide range of lake sizes (from 20 to 2×10^8 m^2). The results were in fair agreement with other published data for world lakes including those in circum-polar regions. Based on available measurements of CH_4, CO_2, and dissolved organic carbon (DOC) in thermokarst lakes and thaw ponds of the permafrost-affected part of the WSL, we found an inverse relationship between lake size and concentration, with concentrations of GHGs and DOC being highest in small thaw ponds. However, since these small ponds represent only a tiny fraction of the landscape (i.e. ~1.5% of the total lake area), their contribution to the total pool of GHG and DOC in inland lentic water of the permafrost-affected part of the WSL is less than 2%. As such, despite high concentrations of DOC and GHG in small ponds, their role in overall C storage can be negated. Ongoing lake drainage due to climate warming and permafrost thaw in the WSL may lead to a decrease in GHG emission potential from inland waters and DOC release from lakes to rivers.

1. Introduction

Aside from rivers and streams, lakes are also an important source of greenhouse gas (GHG) emission to the atmosphere (Cole *et al* 1994, Tranvik *et al* 2009, Kosten *et al* 2010, Raymond *et al* 2013). Recent field and modeling studies showed that methane emissions from Arctic thermokarst lakes are significant and could increase by two to four times due to global warming (Tan and Zhuang 2015a, 2015b). This may be especially true for the vast Western Siberian Lowland (WSL) that represents a hot spot of CO_2 (Repo *et al* 2007) and CH_4 (Sabrekov *et al* 2014, 2017) emissions from inland waters and covers an area of more than 2 million km^2. A sizeable part of the WSL is represented by frozen peatlands, subject to active thermokarst development. The thermokarst activity on this lowland produces numerous lakes and ponds that have

not been fully inventoried or measured for surface area. These small high-latitude lakes and thaw ponds may turn out to be very important sources of GHG to the atmosphere (Hamilton *et al* 1994, Riera *et al* 1999, Walter *et al* 2006, 2007, Laurion *et al* 2010, Rautio *et al* 2011, Marushchak *et al* 2013, Langer *et al* 2015, Wik *et al* 2016). Although very small lakes and ponds (< 1000 m^2 size) represent only 10% of overall lakes and reservoirs in terms of surface area, they can emit more than 15% of CO_2 and 40% of CH_4 (Holgerson and Raymond 2016). These estimations are based on the power law of lake size distribution using map-based information and satellite imagery (Lehner and Doll 2004, Downing and Prairie 2006) or geo-statistical models (Messager *et al* 2016). McDonald *et al* (2012) were the first to challenge the Downing and Prairie (2006) global estimate for lakes based on the Pareto (power law) distribution. Later, it was argued that the Pareto model overestimates the number and areal coverage of lakes smaller than 10 000–100 000 m^2 (Seekell *et al* 2013, Verpoorter *et al* 2014, Paltan *et al* 2015, Cael and Seekell 2016, Polishchuk *et al* 2017). As a result, the GHG emission flux from these lakes may also be overestimated. The main cause for this is insufficient knowledge of the size- and number-distribution of small (< 5000–$10\,000$ m^2) ponds and lakes. Note that while several papers from the previous decade highlighted large CH_4 emissions from discrete sites (e.g. the work of Walter *et al* 2006, 2007, Walter Anthony *et al* 2014), newer studies have suggested that the overall impact is rather small based on the global landscape context. For example, Stackpoole *et al* (2017) concluded that methane emissions from lakes across Alaska represented a small fraction of the annual aquatic C cycle and that small lakes play a minor role in the GHG budget as they do not cover sufficiently large areas.

Over past decades, climate warming has brought about a sizeable acceleration of thermokarst processes in permafrost regions which has led to an increase in the number of small thaw ponds and thermokarst lakes, as well as concentrations and emissions of methane and CO_2 in these lakes (Karlsson *et al* 2012, 2015, Shirokova *et al* 2013, Walter *et al* 2007, Walter Anthony and Anthony 2013, Walter Anthony *et al* 2014, Sepulveda-Jauregui *et al* 2015). The two major scenarios of thermokarst lake evolution under climate warming and permafrost thaw in western Siberia are (1) drainage of large thermokarst lakes into hydrological networks, which is especially pronounced in discontinuous permafrost zones (Smith *et al* 2005, Riordan *et al* 2006, Polishchuk *et al* 2014) and (2) formation of new depressions, subsidences, and small thaw ponds (< 100–1000 m^2), which is evidenced across all permafrost zones of this region (Pokrovsky *et al* 2011, Shirokova *et al* 2013, Bryksina and Polishchuk 2015). The large lake drainage scenario was first suggested from a comparison of medium-resolution (MR) satellite scenes between 1950 and 2010 in thermokarst regions of western Siberia (Smith *et al* 2005, Riordan *et al* 2006, Polishchuk *et al* 2014).

The evaluation of CH_4 and CO_2 reservoirs and fluxes primarily requires knowledge of lake and pond water surface area (Holgerson and Raymond 2016, Verpoorter *et al* 2014, Downing and Prairie 2006, Abnizova *et al* 2012, Polishchuk *et al* 2015b). Although remote sensing analysis of thermokarst lakes in Siberian and other northern regions confirms the power law of lake size distribution (Karlsson *et al* 2014, Grosse *et al* 2008, Polishchuk *et al* 2015a, 2016b, Viktorov *et al* 2017), the majority of these studies use MR (30 m) Landsat images which do not allow the identification of small lakes and ponds. On the other hand, high-resolution (HR) characterization of lake fraction in the ridge-hollow-lake wetland landscapes (i.e. Terentieva *et al* 2016) does not investigate the detailed small ponds size distribution for permafrost-affected WSL territory. The most recent circum-Arctic Permafrost Region Pond and Lake database (Muster *et al* 2017) deals with a small part of the WSL territory and does not allow quantitative estimation of lake and pond areal coverage and water volume in this region.

It is known that small thaw ponds exhibit concentrations of CH_4, CO_2, and DOC that greatly exceed those in large lakes (Bastviken *et al* 2004, Kortelainen *et al* 2006, Juutinen *et al* 2009, Abnizova *et al* 2012, Kankaala *et al* 2013, Shirokova *et al* 2013, Holgerson 2015, Pelletier *et al* 2015a, 2015b). In order to account for their contribution to overall carbon balance, HR (1–10 m) images have to be combined with MR Landsat data to take into account all lakes, from meter sized to tens of kilometers sized, of a large studied territory (e.g. Polishchuk *et al* 2016a, 2016b. However, the methodology of such integration is not sufficiently developed and does not allow quantification of overall lake numbers and surface areas and GHG and C concentrations and fluxes in inland waters. To fill in this gap, the primary goal of this study was to develop an approach for integrating HR and MR image data into the assessment of lake count and surface coverage for the full extent of lake sizes encountered in western Siberia.

The second goal of this study was to evaluate the total amount of CH_4, CO_2 and carbon in thermokarst lakes of western Siberia using the lake and pond inventory and available data on C concentration in typical thermokarst lakes of the region. In continuous and discontinuous permafrost zones of western Siberia, the smallest thaw ponds (100–1000 m^2) and depressions (1–100 m^2) exhibit an order of magnitude higher concentration of CO_2, up to two orders of magnitude higher methane concentration, and a factor of three to ten higher concentrations of DOC and metals (Pokrovsky *et al* 2011, 2013, 2016, Shirokova *et al* 2013). As such, even with their small contribution to the total lake surface area, these small bodies of water may display carbon storage and GHG flux to the atmosphere comparable to those of large and

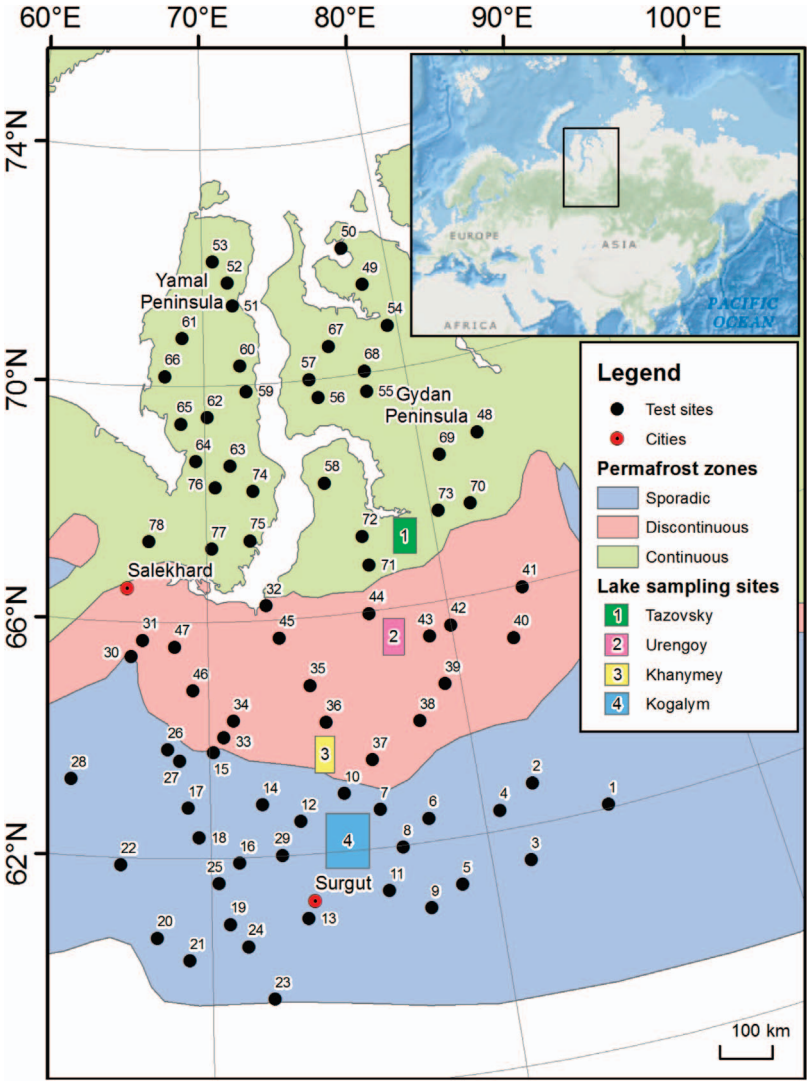

Figure 1. Scheme of location of TSs where Kanopus-V images were available for the permafrost-affected part of western Siberia. Landsat-8 images covered the full territory of permafrost-affected WSL (1.05 million km^2).

medium lakes. We anticipate that the knowledge of GHG and DOC distribution in thermokarst water bodies of the permafrost-affected part of WSL territory combined with known trends of lake and thaw pond area evolution over past decades should allow foresight as to the potential for CH_4 and CO_2 emission into the atmosphere and for the lateral export of DOC to rivers from the lentic aquatic ecosystems of western Siberia.

2. Study site and methods

2.1. Thermokarst lakes and ponds of western Siberia

The WSL is comprised of taiga, forest-tundra, and tundra biomes. Permafrost is abundant north of 60°N, changing from sporadic to discontinuous and continuous northward (figure 1). The climate is humid semi-continental with mean annual temperatures ranging from −2.8 °C in the south of the cryolithozone (Surgut region) to −10.4 °C in the north (Gyda Peninsula). The annual precipitation ranges from 600 mm in the south to 350 mm in the north. Peat thickness ranges from 1 to 3 m and is not directly linked to the latitude (Kremenetski *et al* 2003). The bogs of the region were subjected to freezing during the Subboreal period (~4500 y.a). After the increase in temperature and precipitation during the Subatlantic period (2500 y.a.), the thermokarst started (Ponomareva *et al* 2012, Pastukhov *et al* 2016). It produced thaw ponds and thermokarst lakes that were formed due to progressive thawing of frozen peat rich in ice (Pokrovsky *et al* 2011, Grosse *et al* 2016). On flat watershed divides, which dominate the territory (palsa peat bog and polygonal tundra), the lakes are subjected to a natural cycle of growth and draining which is well established in the WSL (Kirpotin *et al* 2011) but is also evidenced in other parts of the circum-Arctic zone (Hopkins 1949, French 1996). Because of the homogeneous nature of the surrounding substrate (Quaternary clays and sands of fluvio-glacial and lacustro-glacial origin underlying the surface peat

deposits), the thermokarst lakes are generally round in shape. As such, all the lakes and thaw ponds inventoried in this work are considered as having a thermokarst origin. While satellite imagery cannot resolve the origin of small ponds, our terrestrial observations in addition to the very high number of small ponds suggest these ponds were formed after thermokarst subsidence rather than remaining in the basin following large lake drainage.

The range of thermokarst lake and thaw pond sizes in the permafrost-affected part of the WSL is from a few m^2 to hundreds of km^2 (Manasypov *et al* 2014). For convenience, we will distinguish between large lakes ($>10\,000\ m^2$ or 1 ha), small lakes ($500–10\,000\ m^2$), and very small thaw ponds ($<500\ m^2$). This conventional distinction is based on hydrochemical and gas regimes of lakes and ponds; there is an abrupt rise of DOC, CO_2, and CH_4 in water bodies smaller than $500\ m^2$ (Pokrovsky *et al* 2011, 2013, Shirokova *et al* 2013, Manasypov *et al* 2014, Polishchuk *et al* 2015b). This classification is also consistent with that of Holgerson and Raymond (2016) who considered lakes $<1000\ m^2$ as very small water bodies. Muster *et al* (2017) followed the distinction of Rautio *et al* (2011) and defined ponds as bodies of standing water with a surface area smaller than $10\,000\ m^2$.

2.2. Sampling and analyses

Water samples were collected from a PVC boat for large lakes or directly from the lake center for small (<50 m diameter) water bodies (thaw ponds) from the middle of the water column. The sampling was performed during July and August from 2010–2014 (Pokrovsky *et al* 2013, 2014, 2016, Shirokova *et al* 2013, Manasypov *et al* 2014, 2015, Pavlova *et al* 2016, Loiko *et al* 2017) and in August 2015 and 2016 (this study). The typical depth of sampling was between 0.5 and 0.25 m depending on the lake depth (see section 3.3 below). A full list of collected lakes and relevant physico-geographical parameters together with the measured GHG and DOC is given in table S1 of the supplementary information available at stacks.iop.org/ERL/13/045002/mmedia. For GHG analyses, unfiltered water was sampled in 25 m L serum bottles that were closed without air bubbles using vinyl stoppers and aluminum caps and immediately poisoned by adding 0.2 ml of saturated $HgCl_2$ using a two-way needle system. In the laboratory, a headspace was created by displacing approximately 40% of water with N_2 (99.999%). Two 0.5 m L replicates of the equilibrated headspace were analyzed for their concentrations of CH_4 and CO_2, using a Bruker GC-456 gas chromatograph equipped with flame ionization and thermal conductivity detectors. After every ten samples, a calibration of the detectors was performed using air liquid gas standards (i.e. $CH_4 = 145$ ppmv and $CO_2 = 3000$ ppmv). Duplicate injections of the samples showed that results were reproducible within $\pm5\%$. The specific gas solubility for CH_4 and CO_2 (Weiss 1974) were used in the calculation of the total CH_4 and CO_2 content in the vials, which was then recalculated to μmol/L of the initial waters.

For DOC analyses, collected waters were filtered onsite in pre-washed 30 mL polypropylene Nalgene® bottles through single-use Minisart filter units (0.45 μm pore size, Sartorius, acetate cellulose filter). The first 20 ml of filtrate were discarded. Blanks were used to control the level of contamination induced by sampling and filtration. DOC blanks of filtrate never exceeded 0.1 mg L^{-1} which is quite low for the organic-rich pore waters sampled in this study (i.e. 10–100 mg L^{-1} DOC). DOC was analyzed using a Carbon Total Analyzer (Shimadzu TOC VSCN) with an uncertainty better than 3% (see Prokushkin *et al* 2011 for methodology).

2.3. Source and description of satellite imagery

Satellite imagery from the Landsat-8 Operational Land Imager (30 m MR) [available at the USGS Global Visualization Viewer: http://glovis.usgs.gov] together with HR (2 m)) Kanopus-V scenes (available at the Roscosmos website: http://eng.ntsomz.ru/) were used to map the lake distribution over the full territory of permafrost-affected WSL (figure 1). We used MR Landsat-8 images collected at the end of July–beginning of August 2013–2014. HR Kanopus-V images were collected during summers 2013–2015. This free-ice period corresponds to the minimal coverage of the territory by lakes and minimal seasonal variation of lake water levels. A combination of images from the two years was necessary because a single year's observation could not provide full coverage of the territory.

For the entire permafrost-affected WSL territory of 1.05 million km^2, we used a superposition of 134 MR images. Images were treated using standard tools of ArcGIS 10.3 software (Kennedy *et al* 2013). For automatic identification of lakes we used the Fmask algorithm (Zhu *et al* 2015). It allows resolving the lakes even with some cloud coverage and uses several spectral ranges of Landsat-8 using a set of empirical spectral indexes. As input data we used the intensity of the upper atmosphere reflectance and the brightness temperature presented as nominal units of pixel brightness. First, for the mosaic of Landsat-8 imagery, cloud masks were defined for individual images. Then the cloud masks were removed from the images and replaced by cloud-free fragments taken from the adjacent images during the same period of observation. The minimal pixel on the MR image was $30 \times 30\ m^2$, thus limiting the minimal lake size of 0.5 ha or $5000\ m^2$. This corresponds to six pixels of $30\ m \times 30\ m$ ($900\ m^2$), which is sufficient for reliably distinguishing lakes from background noise.

A two-stage procedure was developed to separate thermokarst lakes and thaw ponds from other water objects. First, we masked coastal zones and rivers, based on vector layers of OpenStreetMap and State Water Register (http://textual.ru/gvr/). Second, we superposed this mask on a raster layer of

Table 1. Characteristics of the TSs and HR satellite images.

Permafrost zone	Number of TS	Identification in figure 1	Average area of TS, km^2	Period
Sporadic	29	1–29	2845	2013–2014
Discontinuous	18	30–47	3125	2013–2014
Continuous	31	47–78	3109	2013–2015

recognized water objects forming a layer of lakes. The uncertainty of lake surface area measurement using Landsat-8 for lakes with sizes larger than 10^5 m^2 is 3.5% and for lakes larger than 2×10^4 m^2 is 7% (Bryksina and Polishchuk 2013, Kornienko 2014).

It is important to note that thermokarst lakes and thaw ponds of western Siberia are different from glacial lakes of other boreal and subarctic regions. The latter are often developed on moraine and crystalline rocks and located within non-isometric elongated basins that were formed by glacier movement. In contrast, thermokarst lakes in palsa bogs of western Siberia occurring within frozen 1–3 m peat deposits are rarely oval and are usually round and isolated (Kirpotin *et al* 2009, 2011, 2014, Shirokova *et al* 2013, Pokrovsky *et al* 2014). According to our field observations and detailed lake mapping over 950 km latitudinal gradient of western Siberia, the fraction of lakes with an irregular shape is less than 10% (Pokrovsky *et al* 2011, Manasypov *et al* 2014, 2015, Polishchuk *et al* 2017). For this reason, the influence of the irregularity of the lake border on the determination of the total lake area can be neglected. This is also confirmed by a study of the tortuosity of thermokarst lake border lines demonstrating that the deviation from circumference in lakes of sporadic, discontinuous and continuous permafrost zones produces less than 5% uncertainty on total lake area evaluation by Landsat-8 (Polishchuk and Polishchuk 2012).

HR Kanopus-V images were used for the quantification of small lakes and very small thaw ponds. For the reliable identification of lakes, at least five pixels are necessary. The minimal pond size inferred from the Kanopus-V images was 20 m^2 as the spatial resolution of 2 m yielded a pixel size of 4 m^2 allowing the required five pixels to be distinguished on the 20 m^2 area. The scenes were processed using ArcGIS 10.3 within 78 test sites (TSs), which were evenly distributed over sporadic, discontinuous, and continuous permafrost zones of the WSL (figure 1). The characteristics of these TSs are given in table 1. The number of lakes and ponds on each TS ranged from 97–2583. All TSs had similar sizes (30 km^2) and covered approximately 2000 km^2 which represents 0.002% of the overall permafrost-affected territory of the WSL.

We used a binary classification algorithm in ArcGIS 10.3 analogous to the 'density slice' method used by Muster *et al* (2017). This algorithm is based on the visual detection of certain threshold values of spectral brightness that allow us to distinguish two object classes: 'water' and 'not water'. The threshold value had to be selected individually for each TS due to differences in illumination, acquisition geometry, and different sensor spectroradiometry. The panchromatic imagery exhibited a strong contrast between water surface and the surrounding vegetation which allowed an adequate selection of threshold values needed for classification. The submerged moss and macrophytes were not detected and non-submerged moss and plants along the lake coasts had no influence on lake water surface area.

2.4. Building the integral diagrams of lake number and area distribution in a wide range of lake sizes

To build the diagrams of lake distribution in a wide range of lake sizes, we used 21 partial ranges of lake size taken within a logarithmic scale, i.e. 20–50 m^2, 50–100 m^2, 100–200 m^2, 200–500 m^2 and so on until 200 000 000 m^2. To combine MR and HR images we developed a three-step procedure. First, we constructed diagrams for the number and area distribution of all thermokarst lakes detectable on the MR images. Then, we built similar diagrams for small thermokarst lakes and very small thaw ponds using HR images of the 78 TSs across the permafrost-affected part of WSL. At this stage, the total number and area of lakes located within the TSs were extrapolated to the full territory of the permafrost-affected part of WSL, as described below.

Considering the values of lake numbers and areas in the lake size intervals suitable for Landsat-8 mapping as the most reliable, we required that within the lake size intervals where Landsat-8 and Kanopus-V images overlap, the lake number and area determined from HR scenes on TSs were to be equal to values extrapolated to the full studied territory. We believe that such extrapolation is valid because the TSs are evenly distributed across the permafrost-affected part of the WSL. The extrapolated (calculated) values for the total number ($_{\mathrm{Ncj}}$) and total lake area ($_{\mathrm{Scj}}$) in each jth interval of HR images-based histogram were obtained from:

$$N_{cj} = N_{ej} \times K \quad (1)$$

$$S_{cj} = S_{ej} \times K \quad (2)$$

where N_{ej} and S_{ej} are the total number and area of lakes, respectively, that are experimentally determined based on HR scenes of all TSs, j is the number of intervals of the histogram (figure 2), and K is the empirical extrapolation coefficient which was averaged over all lake sizes and therefore independent in terms of size range. Finally, we combined primary MR and HR histograms into integral histograms of lake numbers and overall areas. These histograms included lakes and small and very small thaw ponds spread over seven orders of magnitude in size.

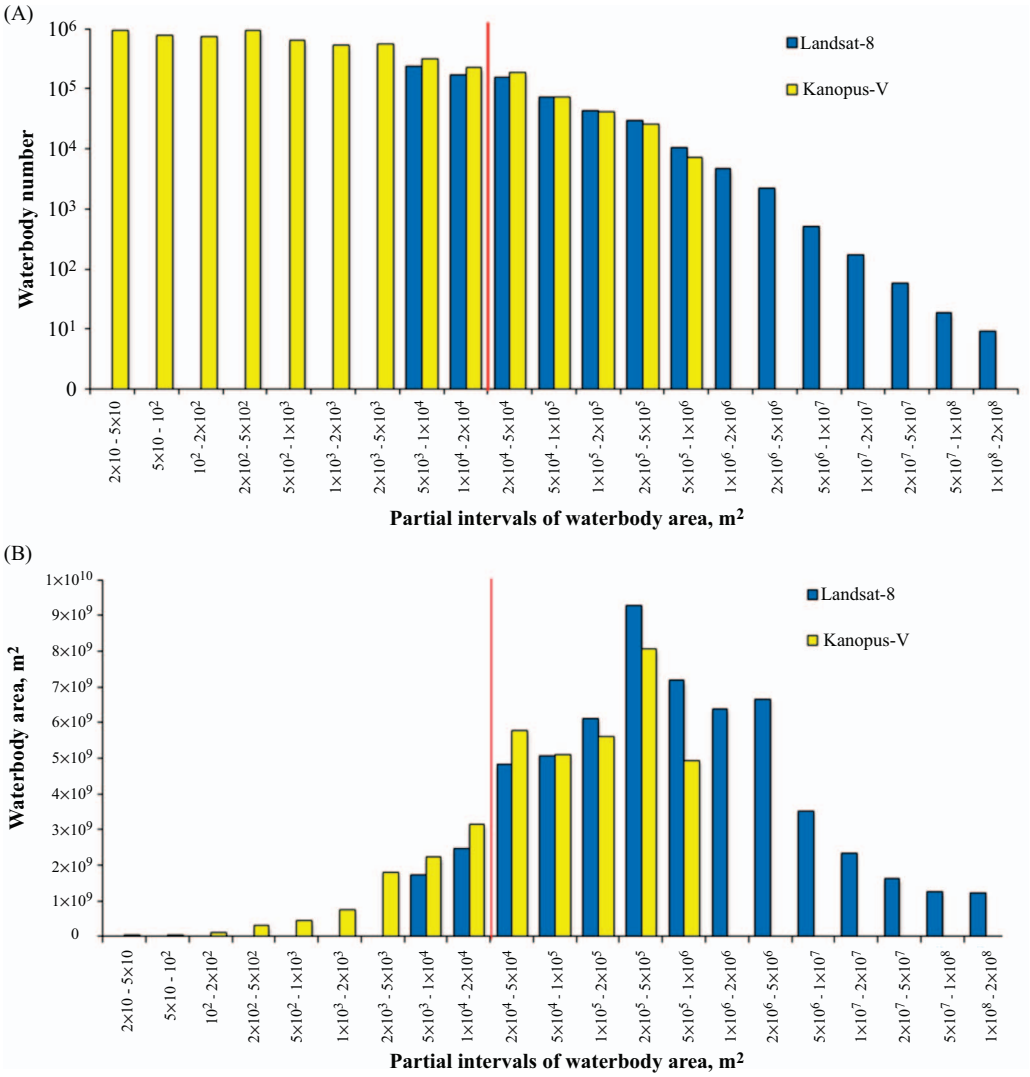

Figure 2. The illustration of MR (Landsat-8, blue columns)–HR (Kanopus-V, yellow columns) number of lakes (*a*) and area (*b*) histogram coupling within the total range of 20 to 2×10^8 m^2 with an overlap in the range of 5×10^3 to 10^6 m^2. Red vertical line marks the point of integration (stitching) of HR and MR-based lake diagrams.

The uncertainty of extrapolating data from the 78 TSs to the whole territory of the permafrost-affected part of the WSL was evaluated via a comparison between data of HR and MR in the lake size interval where the HR and MR scenes overlap (figure 2). Using the number of lakes in the seven intervals of superposition, we found the relative difference in lake numbers using equation 3:

$$\beta_i = (m_i - n_i)/n_i \quad (3)$$

where m_i and n_i represent the number of lakes in the ith overlapped interval, determined using HR and MR images, respectively. In this equation, n_i is chosen as a reference number given that HR images were treated for the full territory of the permafrost-affected part of WSL. The average β_i value of the seven overlapped intervals was equal to 15% which is acceptable for lake size distribution estimation.

3. Results and discussion

3.1. Lake number and area in a wide range of lake sizes, from 20 to 2×10^8 m^2.

The MR images allowed resolving lakes of the minimal size of 5000 m^2 corresponding to six pixels which is necessary to distinguish the lakes from the surrounding landscape. The total number of lakes ranging from 5000 m^2 to 2×10^8 m^2 was 727 700 with a total water area of 60000 km^2. The histograms of lake numbers and lake area distribution over discrete size ranges are given in the blue columns in figures 2(*a*) and (*b*), respectively. The HR (Kanopus-V) scenes were used to quantify the number and areas for small thaw ponds. The empirical extrapolation coefficient (equations 1 and 2) was calculated as an average of the ratio of lake number and area determined by MR scenes for the entire permafrost-affected part of the WSL territory to the total lake number and area from all HR images (at all TSs) in each lake size interval where

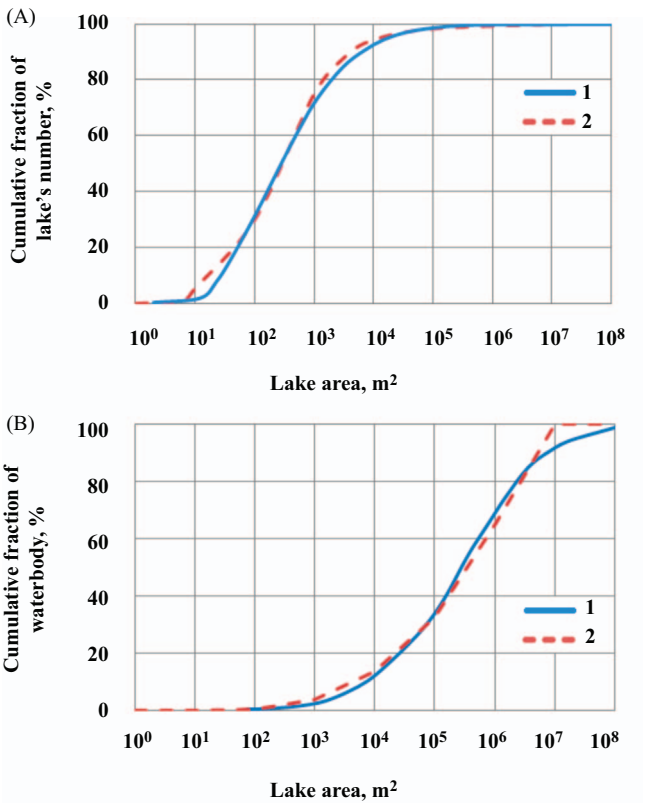

Figure 3. Comparison of the cumulative fraction of number of lakes (*a*) and lake/pond area (*b*) as a function of lake area in the WSL obtained by a combination of MR Landsat-8 and HR Kanopus-V scenes (this study, blue line 1) and all circum-Arctic permafrost region obtained by Muster *et al* (2017) shown by red dashed line.

the HR and MR histograms overlap. The histograms have a seven-interval wide overlap range from 5000 to 10^6 m^2 (figure 2). The extrapolation coefficient values calculated from the data on the number and area of lakes were equal to 85 and 86 respectively. Thus, $K = 85.5$ was defined as an arithmetic mean of these values.

The calculated numbers and total areas of lakes in each interval of lake size using equations 1 and 2 yielded the diagrams of small lakes and very small thaw ponds distribution on the territory, shown as yellow columns in figures 2(*a*) and (*b*) for the lake size range of 20–10^6 m^2. The integration (stitching) of HR and MR-based lake diagrams can be performed at the lake size of 20 000 m^2 with a typical uncertainty on lake determination at 7% (Bryksina and Polishchuk 2013). This point is shown in figure 2 as a red vertical line. This last step of integrated histograms yielded a lake size and area distribution between 20 and 2×10^8 m^2 so that lakes smaller than 2×10^4 m^2 were processed using HR scenes, and the lakes >20 000 m^2 were treated from MR images.

The total number of lakes was equal to 8.7 million and their total area was 6.4×10^{10} m^2. Very small thaw ponds (< 500 m^2) provided 44.2% of total lake numbers, but their area contributed to less than 0.1% of total area coverage. Big lakes (>10 000 m^2) which accounted for only 9.1% of lake numbers provided 91.1% of all lake areas.

3.2. Comparison of lake inventory in western Siberia with other studies

The number of lakes and lake area–lake size distribution diagrams obtained in this work for the permafrost-affected part of WSL are in fairly good agreement with the inventory of all lakes of the circum-Arctic permafrost region (Muster *et al* 2017); deviation between the two estimations does not exceed several percent (figure 3). A comparison with the world lake database of Cael and Seekell (2016) is shown in figure 4 where empirical distribution lakes in Sweden and throughout the world are shown. It can be seen that for lakes smaller than 10^4–10^5 m^2, at both the planetary and regional (WSL, Sweden) level, there is a sizeable difference between the results of direct measurement and calculation from the power law of lake distribution. Specifically, the power law extrapolation strongly overestimates the small lake number compared to empirical data. As a result, the use of power law can also lead to the overestimation of water and solute amounts in small lakes and very small thaw ponds. Indeed, a plot of the relative contribution of lakes of different size to the total area of lakes demonstrates sizeable differences in the fraction of small lakes calculated by Holgerson and Raymond (2016) for the whole planet and our direct measurements of very small thaw ponds in the permafrost-affected part of the WSL territory (figure 5). The two dependences have a generally similar shape and lakes having an

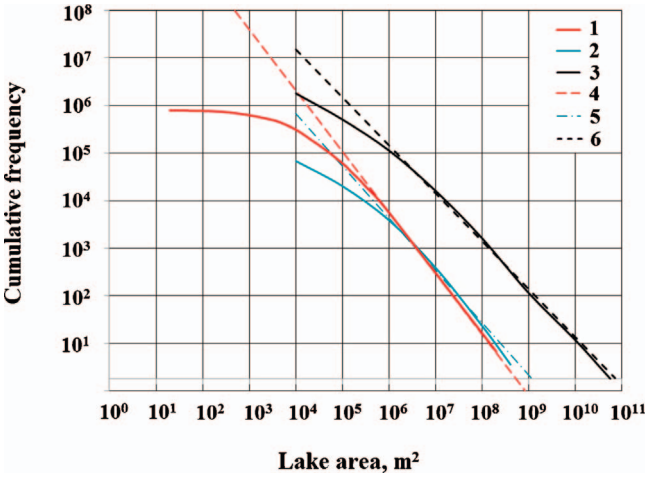

Figure 4. Relationship between the cumulative frequency (the number of lakes versus lake area) of lakes and the lake surface area for the whole territory of WSL (this study, solid red line 1), in comparison with lake distribution in Sweden (solid blue line 2, Cael and Seekell (2016) and in the world (solid violet line 3, Cael and Seekell 2016). The dotted and dashed lines represent power law approximation of western Siberia (red line 4), Sweden (blue line 2), and the whole world (violet line 6).

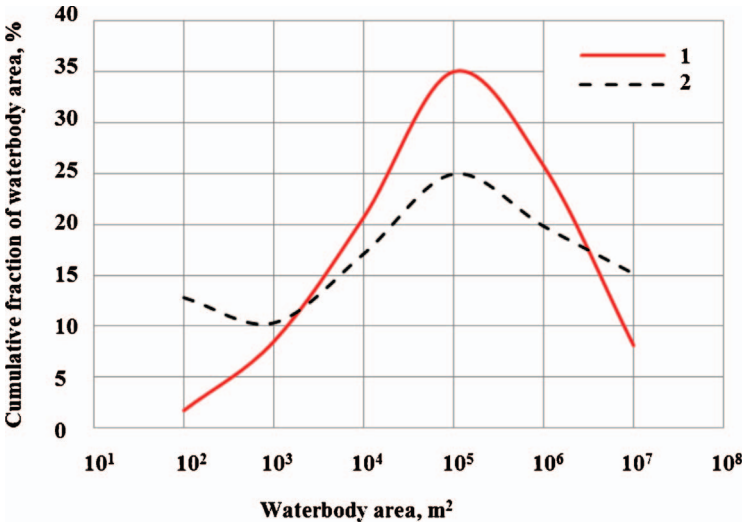

Figure 5. Comparison of the relative contribution of lakes of different size to the total area of lakes, as a function of waterbody area, in western Siberia (red line 1, WSL, this study) and in the world (dashed black line 2, Holgerson and Raymond 2016).

area of 10^5 m^2 provide maximal contribution to the total areal coverage. However, significant differences are pronounced for small water bodies (< 1000 m^2); the relative contribution of lakes evaluated by Holgerson and Raymond (2016) for the world is several times higher than that directly measured in western Siberia. For very small ponds of 100 m^2, this difference is a factor of 6.5. As such, the estimation of total concentrations and emissions of CH_4 and CO_2 from small lakes on a worldwide scale, performed based on Monte Carlo numerical modeling using the Pareto power law (Holgerson and Raymond 2016), cannot be applied to very small thaw ponds of western Siberia. In the WSL direct remote sensing using HR images from 78 TSs allows for a more rigorous lake and pond inventory and thus provides a solid basis for the evaluation of GHG and carbon pools.

It is important to note that the use of Muster *et al*'s (2017) Pond and Lake circum-Arctic database for the WSL territory is not possible. In the work by Polishchuk *et al* (2017), only two sites (Central Yamal and the Surgut region) were inventoried where lake coverage (15%–20%) was much higher than that of the total WSL permafrost-affected zone (5%–10%). In the southern part of the WSL cryolithozone, within the peatland 'Surgutskoe Polesye' of the northern taiga biome (61.5–63°N), the proportion of open water ecosystems is around 19% based on HR (1–3 m) Google Earth inventory (Terentieva *et al* 2016). However, the average limnicity of the permafrost-affected part of the WSL assessed in this study is consistent with values reported in a similar context for two peat plateau areas of northeast European Russia (7%–13.6%, Sjöberg *et al* 2013) and the recent

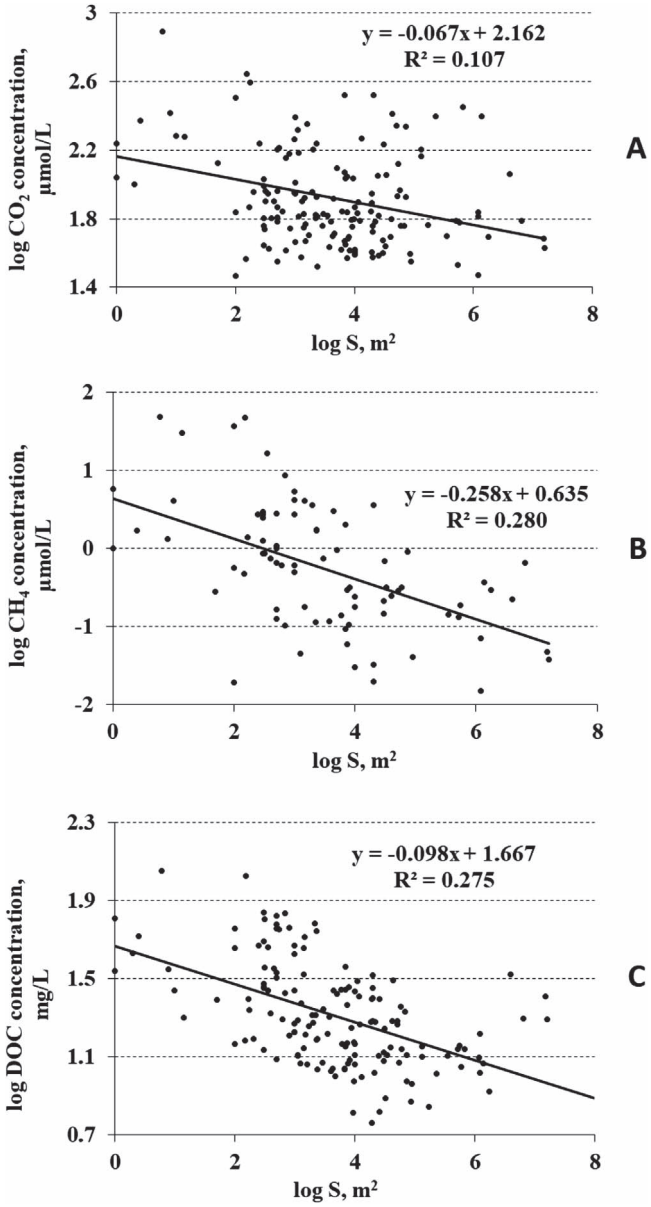

Figure 6. Concentrations of CO_2 (*a*), CH_4 (*b*) and DOC (*c*) in thaw ponds and thermokarst lakes of western Siberia (61–67° N) as a function of the water body area based on field sampling in July–August 2012–2016.

evaluation of lake area density based on geo-statistical modeling (Messager *et al* 2016).

3.3. Calculations of CH_4, CO_2, and DOC pools in small thermokarst lakes and very small thaw ponds of western Siberia

To estimate the amount of GHG and dissolved carbon in lakes of the permafrost-affected part of the WSL, published and new collected concentrations of DOC, CO_2, and CH_4 in 146 thermokarst lakes north of the permafrost boundary were used (Pokrovsky *et al* 2013, 2014, 2016, Shirokova *et al* 2013, Manasypov *et al* 2014, 2015, 2017, Pavlova *et al* 2016, Loiko *et al* 2017, table S1 of the supplementary information). The CO_2 and CH_4 concentrations in small ($< 500\ m^2$) thaw ponds range from 29–778 μmol CO_2 L^{-1} and 0.02–47 μmol CH_4 L^{-1} with average values equal to 172 and 9 μmol L^{-1}, respectively. This is significantly ($p < 0.05$) higher than the range of CO_2 and CH_4 in thermokarst lakes $>500\ m^2$; 29–332 with an average of 92 μmol L^{-1} and 0.02–8.6 with an average of 0.98 μmol L^{-1}, respectively, as illustrated in figures 6(*a*) and (*b*).

The DOC concentration in ponds is a factor of 1.5–2.0 higher than that in lakes (figure 6 (*c*)). Note that the ratio of CO_2 to CH_4 decreases with the decrease in water body area (figure 7) and that this is consistent with the global world trend (Holgerson and Raymond 2016). The concentrations of CO_2, CH_4, and DOC were not found to be significantly ($p < 0.05$) dependent on latitude across the WSL permafrost-affected zone surface waters, soil solutions, and suprapermafrost waters (Manasypov *et al* 2014, Raudina *et al* 2017). For this reason, as a first approximation, we will

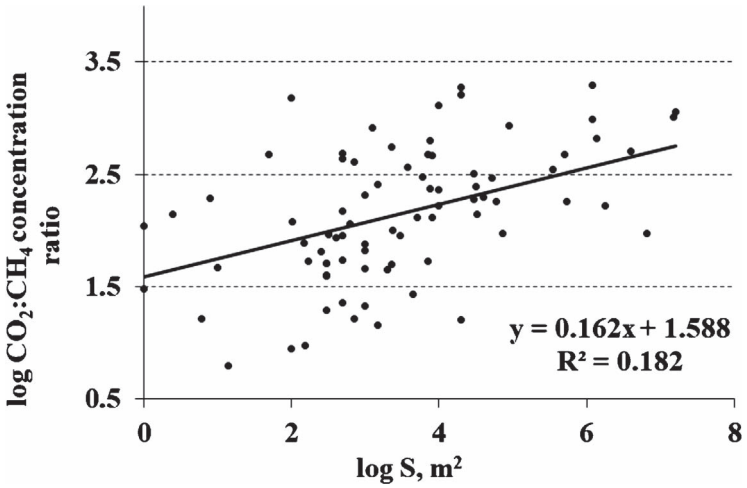

Figure 7. A decrease of CO_2 to CH_4 concentration with decrease of water body area. The relative role of CH_4 is one to two orders of magnitude higher in very small thaw ponds compared to thermokarst lakes.

Table 2. Distribution of CH_4, CO_2, and DOC total amounts among lakes and ponds of different size across the WSL (1.05 million km^2). Uncertainty is estimated between 15% and 30%.

Lake area range, m^2	CH_4, t	CO_2, t	DOC, t	Lake area, km^2
10^1-10^2	6	340	1452	104
10^2-10^3	17	1790	12380	846
10^3-10^4	58	9520	75270	4278
10^4-10^5	192	31700	251000	12360
10^5-10^6	369	60900	482000	22500
10^6-10^7	275	45400	358900	16600
10^7-10^8	87	14300	113100	5222
Total	1004	164000	1294000	61900

Table 3. The distribution of fraction of CH_4, CO_2, and DOC amounts over seven ranges of lake size in the WSL.

Lake area range, m^2	CH_4, %	CO_2, %	DOC, %	Lake area, %
10^1-10^2	0.67	0.22	0.12	0.17
10^2-10^3	1.79	1.17	1.03	1.37
10^3-10^4	6.19	6.24	6.26	6.91
10^4-10^5	20.64	20.82	20.86	19.97
10^5-10^6	39.62	39.98	40.06	36.40
10^6-10^7	29.51	29.78	29.84	26.76
10^7-10^8	9.30	9.38	9.40	8.43

neglect any latitudinal trend in C concentrations in ponds and lakes and consider only lake area as the main controlling parameter of GHG and DOC concentration. It is important to note that the thermokarst lakes and thaw ponds of the WSL are extremely shallow (large lakes are 0.5–1.5 m deep and small thaw ponds are < 0.5 m deep) and are not stratified in temperature. We sampled the surface and bottom layer and have not found any measurable chemical stratification in DOC and CO_2 or O_2. Lakes were fully oxygenated over 0.5–1.5 m depth (Shirokova *et al* 2013, Manasypov *et al* 2015). The latter allowed us to assume the constant profile of CH_4 concentration in the water column.

The depth of WSL thaw ponds and thermokarst lakes depends on the size of the water body (S) and can be approximated by the polynomial equation 4:

$$\text{Depth} = 0.00007 \times S^3 - 0.0049 \times S^2 + 0.1141 \times S - 0.0124 \, (R^2 = 0.552) \quad (4)$$

which is based on field measurements of thaw ponds and lakes of 0.2 to 2×10^7 m^2 (Polishchuk *et al* 2017). This information provides a solid background for the estimation of GHG and DOC reservoirs in the lakes of western Siberia.

The masses of CH_4, CO_2, and DOC in WSL lakes and ponds for seven lake size intervals are listed in table 2. The relative proportions of GHG and DOC in lakes of different size are given in table 3. The maximal contribution to the CH_4 pool in the permafrost-affected part of the WSL is provided by lakes between 10^5 and 10^6 m^2 surface area (figure 8). Lakes larger than 10^4 m^2 provide >90% of the total CH_4 amount whereas the share from small thaw ponds (< 1000 m^2) is only 2%. According to these data, small thaw ponds contribute less to overall CO_2 and DOC levels than to CH_4 level.

3.4. Global consequences of climate warming on pond and lake water GHG emission and DOC lateral export revisited

Remote sensing studies of the permafrost zone of western Siberia demonstrated that the number of newly formed small thermokarst lakes (5000–20 000 m^2) over the past three decades exceeds, by a factor of 20, the number of large lakes which tend to disappear during the same period (Bryksina and Polishchuk 2015). This increase in the number of small and very small thaw ponds over the past few decades was demonstrated through an examination of HR (2 m) Kanopus scenes. Assuming the conservative behavior of carbon in WSL thermokarst lakes and ponds and ignoring the short and long-term dynamics of carbon cycling, the draining of large thermokarst lakes and the appearance of small thaw ponds suggest a sizeable decrease in CO_2, CH_4, and DOC pools in thermokarst water

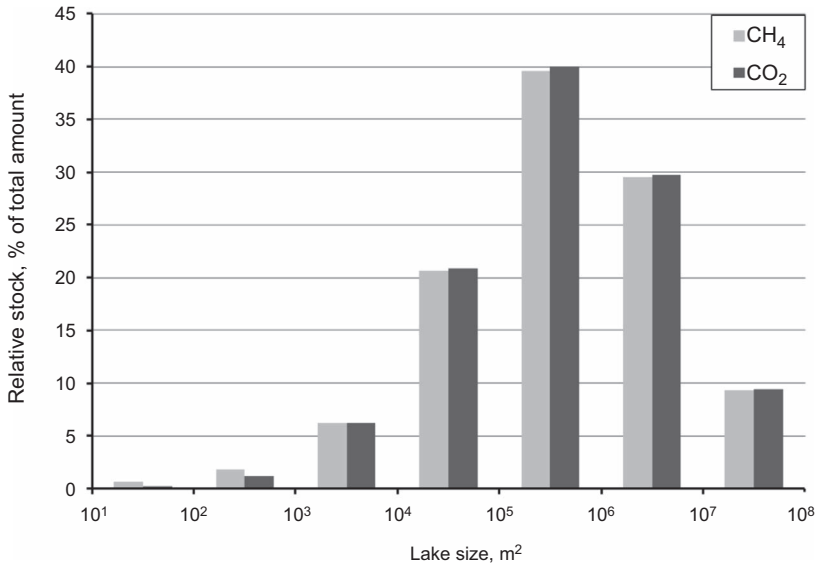

Figure 8. Partial contribution of lakes of different area to the overall concentration of CH_4 (light grey columns) and CO_2 (dark columns) in WSL lakes north of the permafrost boundary.

bodies of the WSL. Thus, a 10%–20% decrease in the area of large (>20,000 m^2) lakes suggested in earlier studies (Smith *et al* 2005, Riordan *et al* 2006, Kravtzova and Bystrova 2009, Shiklomanov *et al* 2013) will lead to a corresponding decrease in CH_4, CO_2, and DOC concentrations in ponds and lakes of the permafrost-affected part of the WSL. At the same time, even a two to threefold increase in the number of small (< 10 000 m^2) lakes and a tenfold increase in very small (< 500 m^2) thaw pond number and area will not produce any sizeable (i.e. >2%) increase in GHG and DOC pools in WSL ponds and lakes. Taken together, the permafrost thaw and climate warming can only decrease the pools of GHG and organic carbon in thermokarst water bodies of western Siberia. Assuming a solely diffusive flux, which is governed by the GHG concentration gradient, this will decrease the CO_2 and CH_4 emission potential to the atmosphere. In addition, the lateral export of DOC from the lakes and ponds to the hydrological network will also decrease. In this regard, our study corroborates the previous results of van Huissteden *et al* (2011) and Kessler *et al* (2012) that thermokarst lake drainage leads to lower GHG emissions.

There are other indications that climate warming and the permafrost thaw may not positively impact the GHG emissions from lentic aquatic ecosystems. For example, the landscape-scale model that included the entire life cycle of thaw lakes in northern Siberia (initiation, expansion, drainage, and eventual re-initiation) demonstrated that methane emissions from thaw lakes in eastern Siberia (Yakutia) are an order of magnitude less alarming than previously suggested (van Huissteden *et al* 2011). Moreover, the use of the Integrated Global System Model demonstrated that, on the whole the Arctic and boreal permafrost-scale increases in atmospheric CH_4 and its radiative forcing (which result from the fact that thawed, inundated emission sources under saturated (anaerobic) soils) are small, particularly when weighed against human emissions (Gao *et al* 2013). Considering the results presented in this work on aerobic (open lake and pond) areas, we believe the overall potential threat of permafrost thaw on GHG emission from Arctic and high latitude boreal permafrost-bearing regions may be overestimated. We do note, however, that detailed mapping of western Siberian wetland complexes (i.e. Peregon *et al* 2008, 2009, Terentieva *et al* 2016) is necessary to integrate available DOC and GHG concentrations and fluxes into a global ecosystem-specific model for this territory. Here, mapping of fine-scale heterogeneity of WSL's wetland landscapes, which is currently possible only for CH_4 emission (i.e. Bohn et al 2007, Glagolev *et al* 2011), will constitute the main challenge for both the DOC and CO_2 inventories. In this regard, quantifying the amount of water and carbon in waterlogged hollows—especially those abundant in the southern part of the permafrost-affected WSL territory (i.e. Terentieva *et al* 2016)—that presumably contain high concentrations of GHG and DOC, may represent a bottleneck of C reservoir inventory in inland waters of the Siberian wetlands. Furthermore, seasonal and daily variability of GHG fluxes in the WSL (Kim *et al* 2011, Sabrekov *et al* 2014) may impede quantitative upscaling of available carbon and GHG concentrations on a year-round basis. For this, landscape-scale modeling of process-based lake biogeochemistry (i.e. Tan *et al* 2017) is needed.

It is further important to note that, despite a net lake area loss due to drainage of large lakes, thermokarst expansion can offset the decrease in GHG emissions and in some regions (i.e. Yedoma Ice Complex)

small lake area increase can increase GHG emissions despite a net loss of large lake area (Walter Anthony *et al* 2016). Moreover, the ultimate response of GHG to the thermokarst lake cycle may be a function of the permafrost type (continuous versus discontinuous), the permafrost carbon stock in terrestrial landscape surrounding lakes (Yedoma, peatland or non-Yedoma mineral soils), the rate of thermokarst expansion, and/or the balance of gross lake area loss versus gain.

Another uncertainty involves the relative role of GHG ebullition versus diffusion which cannot be assessed solely from CO_2 and CH_4 concentrations. Although ebullition is known to dominate over emission in many boreal and Arctic ponds and lakes including those in Siberia (i.e. Walter *et al* 2006, Anthony *et al* 2010) there is no relationship between diffusive emissions and ebullition (Wik *et al* 2016, Sepulveda-Jauregui *et al* 2015). In lakes of permafrost-free regions of the WSL, ebullition strongly dominated over diffusion in the middle taiga zone but was comparable to diffusion in the southern taiga zone (Sabrekov *et al* 2017). As such, the response of GHG emission to frozen peat thaw and permafrost boundary change in the WSL may be more complex than predicted exclusively from GHG total concentrations in lentic waters.

4. Conclusions

A combination of MR (Landsat-8, 30 m) and HR (Kanopus-V, 2 m) satellite imagery of the WSL allowed the quantification of the number and areal coverage of lakes and ponds across the 1.05 million km^2 permafrost-affected territory. The total lake number was equal to 8.7 million with a total area of 6.4×10^{10} m^2. Small and very small thaw ponds (< 1000 m^2) accounted for 44% of the total lake number however their area contributed to less than 0.1% of the total areal coverage. The maximal contribution to the overall CH_4 pool is provided by lakes having 10^5 to 10^6 m^2 surface area. Thus, despite concentrations of DOC and GHG in small thaw ponds that are one to two orders of magnitude higher than those in thermokarst lakes, the share from small thaw ponds is less than 1.5% of the overall CH_4 pool and less than 1% of the CO_2 and DOC pools in lentic waters of the permafrost-affected WSL. A possible consequence of climate warming is that large thermokarst lakes in the permafrost-affected part of the WSL will drain and small thaw ponds will appear. This will clearly decrease, and not increase, the overall CH_4 and CO_2 emission potential from the WSL inland waters and will also decrease possible feeding of streams by DOC from lakes. However, the overall scenario of GHG emissions from inland waters due to permafrost thaw in the permafrost-affected part of the WSL will depend on the evolution of the landscape and changes in the ebullition contribution to total emissions.

Acknowledgments

This work was supported by the RNF (RSCF) grant No 15–17-10009 'Evolution of thermokarst lake ecosystems in the context of climate change' (analyses, interpretation, 50%) and RFBR grants No. 15–45-00075 and 17–55-16008 C NRS-a. We are grateful to three anonymous reviewers for their very constructive remarks. Chris Benker is thanked for the English editing.

ORCID iDs

O S Pokrovsky https://orcid.org/0000-0002-3155-7069

References

Abnizova A, Siemens J, Langer M J and Boike J 2012 Small ponds with major impact: the relevance of ponds and lakes in permafrost landscapes to carbon dioxide emissions *Glob. Biogeochem. Cycles* **26** GB2041

Bastviken D, Cole J, Pace M and Tranvik L 2004 Methane emissions from lakes: dependence of lake characteristics, two regional assessments, and a global estimate *Glob. Biogeochem. Cycles* **18** GB4009

Bohn T J, Lettenmaier D P, Sathulur K, Bowling L C, Podest E, McDonald K C and Friborg T 2007 Methane emissions from western Siberian wetlands: heterogeneity and sensitivity to climate change *Environ. Res. Lett.* **2** 045015

Bryksina N A and Polishchuk Y M 2013 Research of remote measurement accuracy of lake areas using space images *Geoinformatika* **1** 64

Bryksina N A and Polishchuk Y M 2015 Analysis of changes in the number of thermokarst lakes in permafrost of western Siberia on the basis of satellite images *KriosferaZemli* **19** 100–5

Cael B B and Seekell D A 2016 The size-distribution of Earths lakes *Sci. Rep.* **6** 29633

Cole J J, Caraco N F, Kling G W and Kratz T K 1994 Carbon dioxide supersaturation in the surface waters of lakes *Science* **265** 1568–70

Downing J A and Prairie Y T 2006 The global abundance and size distribution of lakes, ponds, and impoundments *Limnol. Oceanogr.* **51** 2388–97

French H M 1996 *The Periglacial Environment* 2nd edn (Harlow: Addison Wesley Longman) p 341

Gao X, Schlosser C A, Sokolov A, Walter Anthony K, Zhuang Q and Kicklighter D 2013 Permafrost degradation and methane: low risk of biogeochemical climate warming feedback *Environ. Res. Lett.* **8** 035014

Glagolev M, Kleptsova I, Filippov I, Maksyutov S and Machida T 2011 Regional methane emission from West Siberia mire landscapes *Environ. Res. Lett.* **6** 045214

Grosse G, Romanovsky V, Walter K, Morgenstern A, Lantuit H and Zimov S 2008 Distribution of thermokarst lakes and ponds at three Yedoma sites in Siberia *Proc. 9th Intern. Conf. Permafrost (June 29–July 3, 2008 Fairbanks, Alaska)* (Fairbanks, USA: Institute of Northern Engineering, University of Alaska Fairbanks) pp 551–6

Grosse G, Goetz S J, McGuire A D, Romanovsky V E and Schuur E A G 2016 Changing permafrost in a warming world and feedbacks to the Earth system *Environ. Res. Lett.* **11** 040201

Hamilton J D, Kelly C A, Rudd J W M, Hesslein R H and Roulet N T 1994 Flux to the atmosphere of CH_4 and CO_2 from wetland ponds on the Hudson-Bay lowlands (HBLs) *J. Geophys. Res.* **99** 1495–510

Holgerson M A 2015 Drivers of carbon dioxide and methane supersaturation in small, temporary ponds *Biogeochemistry* **124** 305–18

Holgerson M A and Raymond P A 2016 Large contribution to inland water CO_2 and CH_4 emissions from very small ponds *Nat. Geosci.* **9** 222–6

Hopkins D 1949 Thaw lakes and thaw sinks in the Imuruk Lake Area, Seward Peninsula, Alaska *J. Geol.* **57** 119–31

Juutinen S, Rantakari M, Kortelainen P, Huttunen J T, Larmola T, Alm J, Silvola J and Martikainen P J 2009 Methane dynamics in different boreal lake types *Biogeosciences* **6** 209–23

Kankaala P, Huotari J, Tulonen T and Ojala A 2013 Lake-size dependent physical forcing drives carbon dioxide and methane effluxes from lakes in a boreal landscape *Limnol. Oceanogr.* **58** 1915–30

Karlsson J M, Lyon S W and Destouni G 2012 Thermokarstlake, hydrological flow and water balance indicators of permafrost change in western Siberia *J. Hydrol.* **464** 459–66

Karlsson J M, Lyon S W and Destouni G 2014 Temporal behavior of lake size-distribution in a thawing permafrost landscape in northwestern Siberia *Remote Sens.* **6** 621–36

Karlsson J M, Jaramillo F and Destouni G 2015 Hydro-climatic and lake change patterns in Arctic permafrost and non-permafrost areas *J. Hydrol.* **529** 134–45

Kennedy M D, Goodchild M F and Dangermond J 2013 *Introducing Geographic Information Systems with ArcGIS: A Workbook Approach to Learning GIS* (New York: Wiley) p 672

Kessler M A, Plug L J and Walter Anthony K M 2012 Simulating the decadal- to millennial-scale dynamics of morphology and sequestered carbon mobilization of two thermokarst lakes in NW Alaska *J. Geophys. Res.* **117** G00M06

Kim H-S, Maksyutov S, Glagolev M V, Machida T, Patra P K, Sudo K and Inoue G 2011 Evaluation of methane emissions from West Siberian Wetlands based on inverse modeling *Environ. Res. Lett.* **6** 035201

Kirpotin S, Polishchuk Y and Bryksina N 2009 Abrupt changes of thermokarst lakes in western Siberia: impacts of climatic warming on permafrost melting *Int. J. Environ. Stud.* **66** 423–31

Kirpotin S *et al* 2011 West Siberian palsapeatlands: distribution, typology, cyclic development, present day climate-driven changes, seasonal hydrology and impact on CO_2 cycle *Int. J. Environ. Stud.* **68** 603–23

Kornienko S G 2014 Assessment accuracy of measurement of the water body area in the permafrost using different spatial resolution satellite imagery *Kriosfera Zemli (Earth Cryosphere)* **18** 86–93

Kortelainen P, Rantakari M, Huttunen J T, Mattsson T, Alm J, Juutinen S, Larmola T, Silvola J and Martikainen P J 2006 Sediment respiration and lake trophic state are important predictors of large CO_2 evasion from small boreal lakes *Glob. Change Biol.* **12** 1554–67

Kosten S, Roland F, Da Motta Marques D M L, Van Nes E H, Mazzeo N, Sternberg L D S L, Scheffer M and Cole J J 2010 Climate - dependent CO_2 emissions from lakes *Glob. Biogeochem. Cycles* **24** GB2007

Kravtzova V I and Bystrova A G 2009 Study of thermokarst lake size in different regions of Russia over last 30 years *Kriosfera Zemli (Earth Cryosphere)* **13** 12–26

Kremenetski K V, Velichko A A, Borisova O K, MacDonald G M, Smith L C, Frey K E and Orlova L A 2003 Peatlands of the West Siberian Lowlands: Current knowledge on zonation, carbon content, and late quaternary history *Quarter. Sci. Rev.* **22** 703–23

Langer M, Westermann S, Walter Anthony K, Wischnewski K and Boike J 2015 Frozen ponds: production and storage of methane during the Arctic winter in a lowland tundra landscape in northern Siberia, Lena River delta *Biogeosciences* **12** 977–90

Laurion I, Vincent W F, MacIntyre S, Retamal L, Dupont C, Francus P and Pienitz R 2010 Variability in greenhouse gas emissions from permafrost thaw ponds *Limnol. Oceanogr.* **55** 115–33

Lehner B and Doll P 2004 Development and validation of a global database of lakes, reservoirs and wetlands *J. Hydrol.* **296** 1–22

Loiko S V, Pokrovsky O S, Raudina T, Lim A, Kolesnichenko L G, Shirokova L S, Vorobyev S N and Kirpotin S N 2017 Hotspots of permafrost thawing enhance organic carbon, CO_2, nutrient and metal release into thermokarst waters *Chem. Geol.* **471** 153–65

Manasypov R M, Pokrovsky O S, Kirpotin S N and Shirokova L S 2014 Thermokarstlake waters across permafrost zones of western Siberia *Cryosphere* **8** 1177–93

Manasypov R M *et al* 2015 Seasonal dynamics of organic carbon and metals in thermokarst lakes from the discontinuous permafrost zone of western Siberia *Biogeosciences* **12** 3009–28

Manasypov R M, Shirokova L S and Pokrovsky O S 2017 Experimental modeling of thaw lake water evolution in discontinuous permafrost zone: role of peat and lichen leaching and ground fire *Sci. Total Environ.* **580** 245–57

Marushchak M E, Kiepe I, Biasi C, Elsakov V, Friborg T, Johansson T, Soegaard H, Virtanen T and Martikainen P J 2013 Carbon dioxide balance of subarctic tundra from plot to regional scales *Biogeosciences* **10** 437–52

McDonald C P, Rover J A, Stets E G and Striegl R G 2012 The regional abundance and size distribution of lakes and reservoirs in the United States and implications for estimates of global lake extent *Limnol. Oceanogr.* **57** 597–606

Messager M L, Lehner B, Grill G, Nedeva I and Schmitt O 2016 Estimating the volume and age of water stored in global lakes using a geo-statistical approach *Nat. Comm.* **7** 13603

Muster S *et al* 2017 PeRL: A circum-Arctic permafrost region pond and lake database *Earth Syst. Sci. Data* **9** 317–48

Paltan H, Dash J and Edwards M 2015 A refined mapping of Arctic lakes using landsat imagery *Int. J. Remote Sens.* **36** 5970–82

Pastukhov A V, Marchenko-Vagapova T I, Kaverin D A and Goncharova N N 2016 Genesis and evolution of peat plateaus in the sporadic permafrost area in the European North-East (middle basin of the Kosyu river) *Earths Cryosphere* **20** 3–13

Pavlova O A, Pokrovsky O S, Manasypov R M, Shirokova L S and Vorobyev S N 2016 Seasonal dynamics of phytoplankton in acidic and humic environment in shallow thaw ponds of western Siberia, discontinuous permafrost zone *Ann. Limnol. Int. J. Limnol.* **52** 47–60

Pelletier L, Strachan I B, Roulet N T and Garneau M 2015a Can boreal peatlands with pools be net sinks for CO_2? *Environ. Res. Lett.* **10** 035002

Pelletier L, Strachan I B, Roulet N T, Garneau M and Wischnewski K 2015b Effect of open water pools on ecosystem scale surface-atmosphere carbon dioxide exchange in a boreal peatland *Biogeochemistry* **124** 291–304

Peregon A, Maksyutov S, Kosykh N P and Mironycheva-Tokareva N P 2008 Map-based inventory of wetland biomass and net primary production in western Siberia *J. Geophys. Res. Biogeo.* **113** G01007

Peregon A, Maksyutov S and Yamagata Y 2009 An image-based inventory of the spatial structure of West Siberian wetlands *Environ. Res. Lett.* **4** 045014

Pokrovsky O S, Shirokova L S, Kirpotin S N, Audry S, Viers J and Dupré B 2011 Effect of permafrost thawing on the organic carbon and metal speciation in thermokarst lakes of western Siberia *Biogeosciences* **8** 565–83

Pokrovsky O S, Shirokova L S, Kirpotin S N, Kulizhsky S P and Vorobiev S N 2013 Impact of western Siberia heat wave 2012 on greenhouse gases and trace metal concentration in thaw lakes of discontinuous permafrost zone *Biogeosciences* **10** 5349–65

Pokrovsky O S, Shirokova L S and Kirpotin S N 2014 *Biogeochemistry of Thermokarst Lakes of western Siberia* (New York: Nova Science) p 163

Pokrovsky O S, Manasypov R M, Loiko S V and Shirokova L S 2016 Organic and organo-mineral colloids of discontinuous permafrost zone *Geochim. Cosmochim.Acta* **188** 1–20

Polishchuk Y, Kirpotin S and Bryksina N 2014 Remote study of thermokarst lakes dynamics in West-Siberian permafrost *Permafrost: Distribution, Composition and Impacts on Infrastructure and Ecosystems* ed O S Pokrovsky (New York: Nova Science) pp 173–204

Polishchuk Y M, Bryksina N A and Polishchuk V Y 2015a Remote analysis of changes in the number and distribution of small thermokarst lakes by sizes in cryolithozone of western Siberia *Izvestia Atmos Ocean. Phys.* **51** 999–1006

Polishchuk Y M, Polishchuk V Y, Bryksina N A, Pokrovskiy O S, Kirpotin S N and Shirokova L S 2015b Methodical issues of evaluating methane capacity in small thermokarst lakes of western Siberian permafrost *Bull. Tomsk Politech. Univ.* **326** 127–35

Polishchuk Y M, Bogdanov A N and Muratov I N 2016a Methodological issues of construction of generalized histograms of lake size-distribution in the permafrost based on the satellite images of middle and high resolution *Mod. Prob. Earth Remote Sens. Space* **13** 224–32

Polishchuk Y M, Muratov I N and Polishchuk V Y 2016b Studying the fields of small thermokarst lakes in the continuous permafrost of western Siberia by high resolution satellite images *Atmos. Ocean. Opt.* **29** 592–7

Polishchuk V Y and Polishchuk Y M 2012 Remote studies of the variability of the shape of coastal boundaries of thermokarst lakes in the territory of West-Siberian permafrost *Study Earth Space* **1** 61–4

Polishchuk Y M, Bogdanov A N, Polischuk V Y, Manasypov R M, Shirokova L S, Kirpotin S N and Pokrovsky O S 2017 Size-distribution, surface coverage, water, carbon and metal storage of thermokarst lakes (>0.5 ha) in permafrost zone of the western Siberia Lowland *Water* **9** 228

Ponomareva O E, Gravis A G and Berdnikov N M 2012 Contemporary dynamics of frost mounds and flat peatlands in north taiga of West Siberia (on the example of Nadym site) *Kriosfera Zemli (Earth Cryosphere)* **26** 21–30

Prokushkin A S, Pokrovsky O S, Shirokova L S, Korets M A, Viers J, Prokushkin S G, Amon R, Guggenberger G and McDowell W H 2011 Sources and export fluxes of dissolved carbon in rivers draining larch-dominated basins of the central Siberian plateau *Environ. Res. Lett.* **6** 045212

Raudina T V, Loiko S V, Lim A G, Krickov I V, Shirokova L S, Istignichev G I, Kuzmina D M, Kulizhsky S P, Vorobyev S N and Pokrovsky O S 2017 Dissolved organic carbon and major and trace elements in peat porewater of sporadic, discontinuous, and continuous permafrost zones of western Siberia *Biogeosciences* **14** 3561–84

Rautio M, Dufresne F, Laurion I, Bonilla S, Vincent W and Christoffersen K 2011 Shallow freshwater ecosystems of the circumpolar Arctic *Ecoscience* **18** 204–22

Raymond P A *et al* 2013 Global carbon dioxide emissions from inland waters *Nature* **503** 355–9

Repo M E, Huttunen J T, Naumov A V, Chichulin A V, Lapshina E D, Bleuten W and Martikainen P J 2007 Release of CO_2 and CH_4 from small wetland lakes in western Siberia *Tellus* **59B** 788–96

Riera J L, Schindler J E and Kratz T K 1999 Seasonal dynamics of carbon dioxide and methane in two clear-water lakes and two bog lakes in northern Wisconsin, USA *Can. J. Fish. Aquat. Sci.* **56** 265–74

Riordan B, Verbyla D and McGuire A D 2006 Shrinking ponds in subarctic Alaska based on 1950–2002 remotely sensed images *J. Geophys. Res.* **111** G04002

Sabrekov A F, Runkle B R K, Glagolev M V, Kleptsova I E and Maksyutov S S 2014 Seasonal variability as a source of uncertainty in the West Siberian regional CH_4 flux upscaling *Environ. Res. Lett.* **9** 045008

Sabrekov A F, Runkle B R K, Glagolev M V, Terentieva I E, Stepanenko V M, Kotsyurbenko O R, Maksyutov S S and Pokrovsky O S 2017 Variability in methane emissions from West Siberia's shallow boreal lakes *Biogeosciences* **14** 3715–42

Seekell D A, Pace M L, Tranvik L J and Verpoorter C A 2013 A fractal-based approach to lake size-distributions *Geophys. Res. Lett.* **40** 517–21

Sepulveda-Jauregui A, Walter Anthony K M, Martinez Crus K, Greene S and Thalasso F 2015 Methane and carbon dioxide emissions from 40 lakes along a north-south latitudinal transect in Alaska *Biogeosciences* **12** 3197–223

Shiklomanov A I, Lammers R B, Lettermaier D P, Polishchuk Y M, Savichev O G and Smith L C 2013 Hydrological changes: historical analysis, contemporary status, and future projections *Regional Environmental Changes in Siberia and their Global Consequences* ed P Ya Groisman and G Gutman (Heidelberg: Springer) pp 111–54

Shirokova L S, Pokrovsky O S, Kirpotin S N, Desmukh C, Pokrovsky B G, Audry S and Viers J 2013 Biogeochemistry of organic carbon, CO_2, CH_4, and trace elements in thermokarst water bodies in discontinuous permafrost zones of western Siberia *Biogeochemistry* **113** 573–93

Sjöberg Y, Hugelius G and Kuhry P 2013 Thermokarst lake morphometry and erosion features in two peat plateau areas of Northeast European Russia *Permafrost Periglac Proc.* **24** 75–81

Smith L, Sheng Y, Macdonald G and Hinzman L 2005 Disappearing Arctic lakes *Science* **308** 14

Stackpoole S M, Butman D E, Clow D W, Verdin K L, Gaglioti B V, Genet H and Striegl R G 2017 Inland waters and their role in the carbon cycle of Alaska *Ecol. Appl.* **27** 1403–20

Tan Z and Zhuang Q 2015a Methane emissions from pan-Arctic lakes during the 21st century: An analysis with process-based models of lake evolution and biogeochemistry *J. Geophys. Res. Biogeosci.* **120** 2641–53

Tan Z and Zhuang Q 2015b Arctic lakes are continuous methane sources to the atmosphere under warming conditions *Environ. Res. Lett.* **10** 054016

Tan Z, Zhuang Q, Shurpali N J, Marushchak M E, Biasi C, Eugster W and Anthony Walter K 2017 Modeling CO_2 emissions from Arctic lakes: Model development and site-level study *J. Adv. Model. Earth Syst.* **9** 2190–213

Terentieva I E, Glagolev M V, Lapshina E D, Sabrekov A F and Maksyutov S 2016 Mapping of West Siberian taiga wetland complexes using Landsat imagery: implications for methane emissions *Biogeosciences* **13** 4615–26

Tranvik L J *et al* 2009 Lakes and reservoirs as regulators of carbon cycling and climate *Limnol. Oceanogr.* **54** 2298–314

van Huissteden J, Berrittella C, Parmentier F J W, Mi Y, Maximov T C and Dolman A J 2011 Methane emissions from permafrost thaw lakes limited by lake drainage *Nat. Clim. Change* **1** 119–23

Verpoorter C, Kutser T, Seekel D A and Tranvik L J 2014 A global inventory of lakes based on high resolution satellite imagery *Geophys. Res. Lett.* **41** 1–7

Viktorov A S, Kapralova V N, Orlov T V, Trapeznikova O N, Arkhipova M V, Berezin P V, Zverev A V, Panchenko E N and Sadkov S A 2017 Thermokarst lake size distribution *Dokl. Acad. Sci. Ser. Geogr.* **474** 625–7

Walter K M, Zimov S A, Chanton J P, Verbyla D and Chapin F S III 2006 Methane bubbling from Siberian thaw lakes as a positive feedback to climate warming *Nature* **443** 71–5

Walter K M, Smith L C and Chapin F S 2007 Methane bubbling from northern lakes: present and future contributions to the global methane budget *Phil. Trans. R. Soc.* **365** 1657–76

Walter Anthony K M, Vas D A, Brosius L, Chapin III F S, Zimov S A and Zhuang Q 2010 Estimating methane emissions from northern lakes using ice-bubble surveys *Limnol. Oceanogr. Methods* **8** 592–609

Walter Anthony K M and Anthony P 2013 Constraining spatial variability of methane ebullition in thermokarst lakes using point-process models *J. Geophys. Res.* **118** 1015–34

Walter Anthony K M, Zimov S A, Grosse G, Jones M C, Anthony P M, Chapin III P M, Finlay F S, Mack J C, Davydov S, Frenzel P and Frolking S 2014 A shift of thermokarst lakes from carbon sources to sinks during the holocene epoch *Nature* **511** 452–6

Walter Anthony K, Daanen R, Anthony P, von Deimling T S, Ping C-L, Chanton J P and Grosse G 2016 Methane emissions proportional to permafrost carbon thawed in Arctic lakes since the 1950s *Nat. Geosci.* **9** 679–82

Weiss R F 1974 Carbon dioxide in water and seawater: the solubility of a non-ideal gas *Mar. Chem.* **2** 203–15

Wik M, Varner R K, Anthony K W, MacIntyre S and Bastviken D 2016 Climate-sensitive northern lakes and ponds are critical components of methane release *Nat. Geosci.* **9** 99–105

Zhu Z, Wang S and Woodcock C E 2015 Improvement and expansion of the Fmask algorithm: cloud, cloud shadow, and snow detection for Landsats 4–7, 8, and Sentinel 2 images *Remote Sens. Environ.* **159** 269–77